ALMA BAND 2(+3) CRYOGENIC DESIGN REPORT

Prepared by: Luca Terenzi

INAF/IASF.bo – Via P. Gobetti 101, I-40129 Bologna. Italy

Checked by: Fabrizio Villa

INAF/IASF.bo – Via P. Gobetti 101, I-40129 Bologna. Italy

ABSTRACT

This report describes a preliminary design of the ALMA band 2+3 cryogenic architecture. The overall design is discussed from the identification of main interfaces and requirements. The main parameters estimates found through a preliminary analysis are shown. At this stage no relevant issues or criticalities are identified, however the main aspects affecting the thermal design in the next development phases are discussed

1   Applicable Documents

AD1.   Cryostat Design Report (FEND-40.03.00.00-007-A-REP)
AD2.   Cryostat Technical Specifications (FEND-40.03.00.00-002-C-SPE)
AD3.   F. Villa, L. Terenzi, *ALMA Band 2(+3) Fore-Optics Design Report*, 2013
AD4.   A.-L. Fontana, *ALMA Band 2+3. WP6: Vacuum windows and Infrared Filters.* 2013

2   Reference Documents

RD1.   *A Science and Design Study for ALMA Band 2, A Proposal to Call CPP/ESO/10/10957/CNI*
RD2.   J.S.Clarke, L.R.D'Addario, *Tests of Materials for Use in Multi-Layer Infrared Filters in Cryogenic Application*, ALMA Memo #269
RD3.   D. Koller, A. R. Kerr, G. A. Ediss, *Proposed Quartz Vacuum Window Designs for*
RD4.   *ALMA Bands 3 – 10*, ALMA Memo #397
RD5.   M. Strandberg et al., *Analysis, Simulation and Design of Cryogenic Systems for ALMA Band 5 Prototype Cartridge*, 2009
RD6.   ITP Engines UK, *ESATAN-TMS Workbench User Manual*, 2012

3 Introduction

The activity described in this report is contained in a study for the design of an ALMA Band 2+3 integrated instrument (RD1). Instruments covering the different frequency bands for the ALMA facility have to be located into a common cryostat, which provides the three main thermal references, down to cryogenic temperatures of about 90, 15 and 4 K. The instruments, in form of cartridges, have a defined volume allocation and some main thermal requirements set. So the cryogenic scheme of the cartridge have to be studied in order to optimize instrumental performance while meeting the requirements.

The preliminary phase of the study, reported in the first draft version of this document, was aimed at verifying that no main limitation of this Band2+3 solution, from the thermal point of view, is expected with respect to a Band2-only instrument.

In this version, the description of a simple thermal model of the system is reported together with main results of the analysis.

4 Overview of the ALMA cryostat

The ALMA cryostat (AD1) is sized in such a way that a sufficient volume allocation is available for the ten different instrument cartridges planned to be seated in it. The cryostat is provided with a three-stage GM cryocooler able to keep the reference flanges temperatures at about 90 K, 12 K and 4.5 K absorbing about 30 W, 8 W and 1W of power respectively.

Typical conductances of the cartridge to the flanges are 1.3 W/K, 0.74 W/K and 0.54 W/K. The instrumental solutions considered in this study will benefit of the two warmest stages at 12 K and 90 K.

Total loads estimated set at these stages for the heat dissipation of the cartridges are reported in the Table 1. These are set as requirements for our system and are split into separated budgets between active electronic devices dissipation, where three cartridges on at a time are considered, and passive load budget which has to take into account all the cartridges mounted.

Stage Temperature	Active load requirement (mW)	Wiring load requirement (mW)
90 K	830	400
12 K	66	95

Table 1 Main power dissipation requirements at the interface with the cryostat

We considered in our study a margin level temperature of the different stage interfaces with the cooler at 95 and 18.5 K.

5 Thermal Layout

We focus here on the proposed scheme for the merged Bands 2 and 3 (Figure 1).

The cryogenic part of the instrument consists of the feed horn and OMT system feeding the first amplification stage at 18 K and then the signal is down converted by means of mixers, fed through standard coaxial cables by the Local Oscillator. The IF signal is then transmitted towards the warm stage at room temperature by means of coaxial cables.
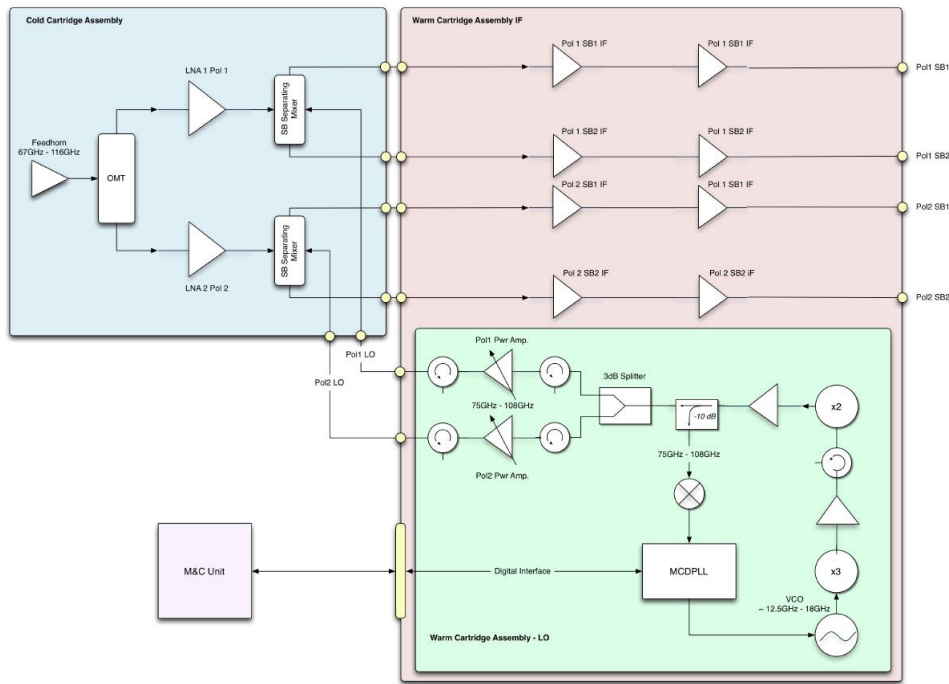
Figure 1 The instrument scheme proposed for the Band2+3 merged solution. The Cold Cartridge Assembly is located in the 15K stage of the cryostat while the Warm Cartridge Assembly is seated at room temperature.

The main thermal interfaces are summarized in the scheme shown in Figure 2. The main active heat load on the colder 18 K stage is coming from the Low Noise Amplifiers. Other relevant thermal interfaces are the radiative heat load, reduced by the dedicated IR filters and by shielding the different stages with MLI sheets.
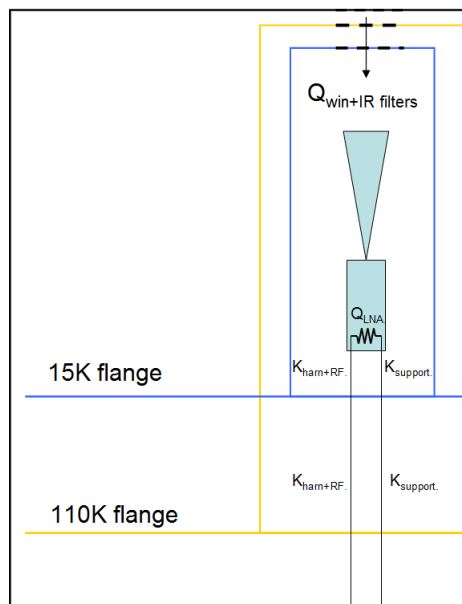

Figure 2 The thermal scheme associated to the instrument layout.

The main conductive interfaces are identified in the mechanical supports of the cold receiver system on the 18 K flange and of the links between the different stages of the cartridges. Other conductances participating to the heat loads on the 18 K and 90 K stages are the coaxial cables transmitting the RF signals and the electrical wires used to bias sensors and amplifiers.

6 Radiative geometrical model

Starting from the instrument scheme and the cold fore-optics design, a sketch of the cartridge has been designed. So a geometrical model derived from this has been built in the ESATAN-TMS environment, in order to evaluate a preliminary balance of the radiative thermal exchanges.

The whole cryostat layout has been simulated as a cylindrical environment of equivalent size, and the same is done for all the intermediate stages. The cartridge has been implemented for simplicity at the center of the cryostat, as a standalone cartridge, which can be nonetheless considered a representative approximation from the thermal radiative point of view. All the intermediate shields are connected to the flanges of the cartridge at the base and have an aperture filled with simulated IR filters on the top. The cold part is represented by the cold optics mirrors and a front end box equivalent to the LNA, OMT and mixer assembly, with the horn at the top. This model has been built to verify that no relevant load is expected at the coldest stage, due to the instrument architecture, so that the extimations and measurements of radiative budget of the cryostat are not affected. On the other hand, the use of standard filters results in a negligible effect of the radiation heat on the cryogenic setup of the cartridge.
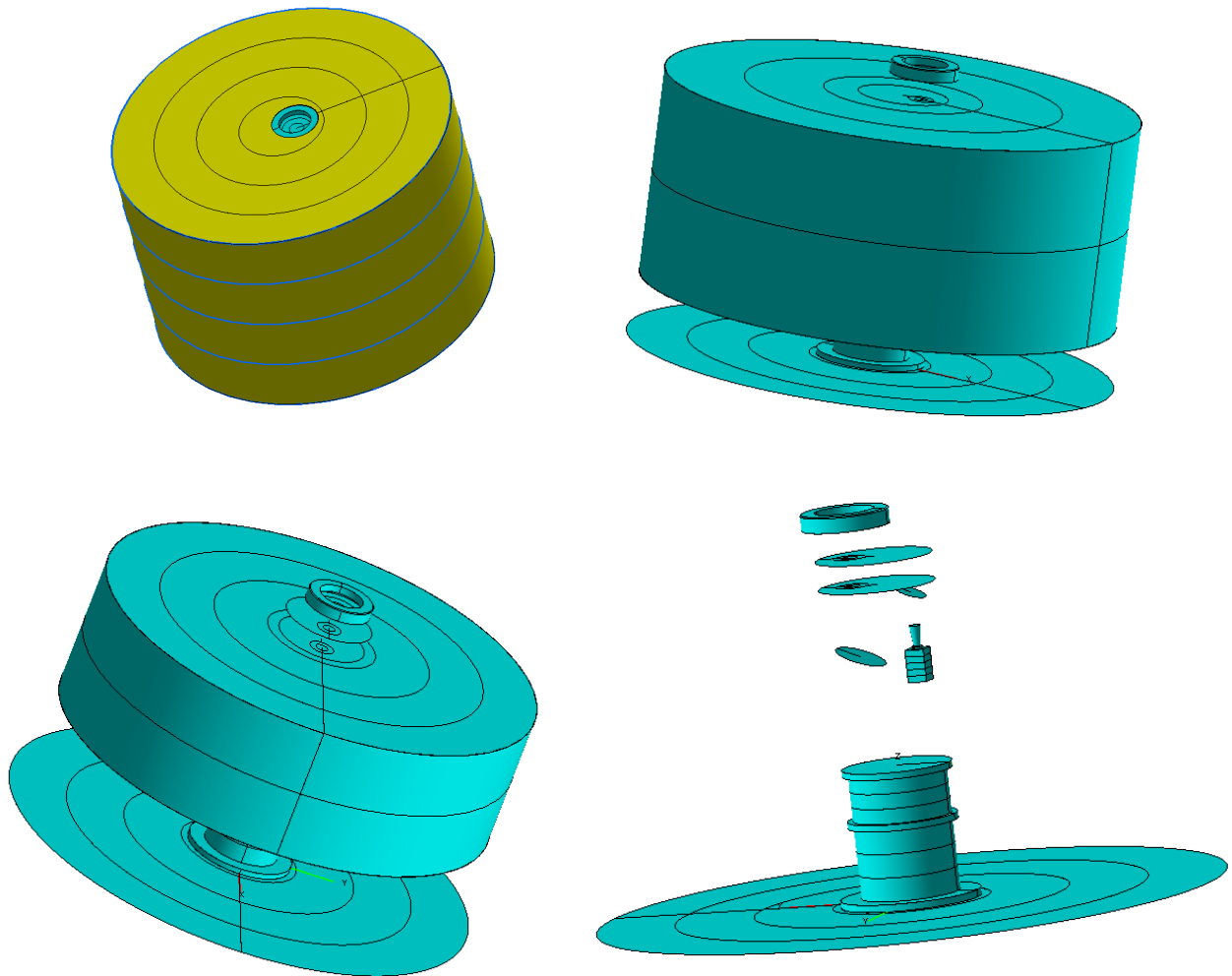
Figure 3 Some views of the geometrical model built to evaluate the radiative exchange factors between the cartridge and the cryostat. Top left: the whole cryostat view. Top right: a view with the lateral and top cryostat shields removed, the window structure and the 90 K shield are visible. Bottom left: a view of the 18 K shield. Bottom right: the inner view of the cartridge, the fron end assembly with the horn and the small mirrors are visible, together with the reference flanges and their cylindrical support structure.

7 Thermal mathematical model

Once the radiative calculator is run, the resulting radiative exchange factors are integrated in the thermal model. The scheme consists of a limited number of materials used:

- all the shields and flanges are made of aluminum together with front end assembly and cold optics
- thermal insulation between the stages of the cartridge is implemented using a thin cylinder of fiberglass
- IR filters are made of PTFE

Conductors not represented in the geometrical model are added together with relevant boundary conditions.

The environment and the outer shield of the cryostat are set as boundary regions at 300 K and 290 K. The two cooler interfaces are represented as boundary conditions on the cartridge flanges at 95 and 18.5 K. The mirrors are considered well connected to the front end assembly, while the main thermal interfaces driving the heat transmission from the front end to the 18 K flange consist of a stainless steel structural frame with an equivalent conductance of 0.05 W/m K, and a set of four K-coaxial cables and 2 V-coaxial cables, with negligible conductance with respect to the mounting structure.

8 Main thermal parameters estimates

In this section, the main results from the model are reported. The list of nodes with temperatures and heat balance is reported in the Appendix 10.1

8.1 Heat Loads

The cryostat design sets requirements on the dissipation of the single cartridges on the differet stages of the cooler as described in Section 4.

The dissipating active devices in the cold stage are low noise amplifiers and mixer diodes. The HEMT technologies taken into account in the study are expected to have a power consumption of the order of few tens of mW. We assumed as a reference a value of 30mW, while for the mixer an estimation of 10 mW is given.

As for the conductive links given by the wires and cables between the 90 and 18 K stage we consider:

- the values reported in the AD3: 20 BeCu (125 μm diameter) wires for LNA bias is consistent with about 3 mW load;
- using 4 30 cm long coaxial cables at the output of the mixer channels and two V band cables feeding the LO input on the front end results in a dissipation of about 18 mW;
- four temperature sensors and two heaters (nominal and redundant) for a possible active control have a limited impact of about 4 mW (20 PhBr AWG36 wires of 15cm length).

The total passive load, due to wires and cables between the 90 K and 18 K stages of the cartridge can then be estimated in about 25 mW.

The same scheme is applied to evaluate the dissipation due to the routing of wires and cables between the 300 K and the 90 K stages. The results show about 25 mW for LNA bias wires, 60 mW for 50cm long coax cables and 15 mW for sensors and heaters wires.

As reported in the table here above the extimation shows a good level of margin within the requirements where to allocate refinements in the process of final design.

Stage	Active load reqs	Active load estimate	Wiring load reqs	Wiring load estimate
90 K	830 mW	--	400 mW	100 mW
12 K	66 mW	40 mW	95 mW	25 mW

The global load estimated from this simplified one cartridge model results in about 9 W on the 90 K stage and 0.8 W on the 18K stage, which, taking into account the different systems simulated, are compliant with the cryostat design model estimating a total of 40 W and 4.85 W respectively.

It has to be noticed that the conductance between the stages is evaluated considering a simple software built-in form of cylinder of G10 fiberglass with a 4mm thickness; the surface through which the heat flows, and then the heat load itself, can be easily reduced by creating custom grooves and empty spaces through the cylinder.

8.2 Absolute temperatures

The temperature distribution of the different parts of the cartridge is shown in the figures below. In particular the coldest region shows a sufficiently low temperature gradient allowing the cold optics and the LNAs, driving the overall instrumental performance, well within their optimal operating range (about 20 K). With a reference cold flange temperature of 18.5 K, in this baseline design the amplifiers and mirrors reach a maximum temperature of about 19.25 K. Also the top part of this stage, at the level of the filter, is reaching about the same temperature, 19.07 K.

The gradient in the 90 K stage is larger due to the higher radiative load and the top part of the shield is resulting about 30 K warmer then the bottom flange.
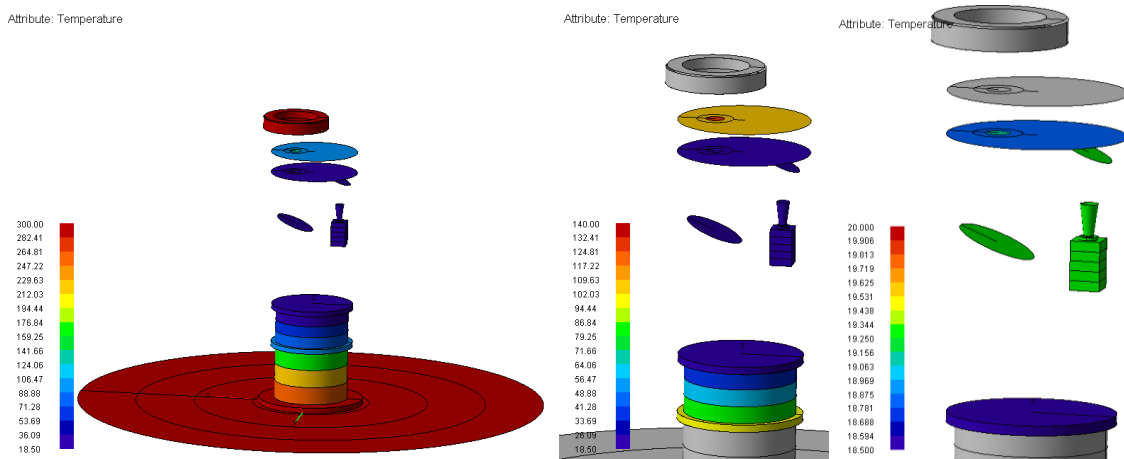
Figure 4 The steady state temperature distribution resulting from the model. The color scale is reduced from the left panel to right in order to have a more and more refined view of the gradients.

8.3 Receiver temperature stability

The main thermal instability time scale is the 1 s period of the cooler cycle. Due to the thermo-mechanical filtering of the flanges and frames into the cryostat and in the different cartridges this fluctuation is reduced up to a small amount of residual fluctuation. In the AD1 some temperature spectra of the cooler cold head and of a reference flange, the band 6 interface, measured during the cryostat qualification tests, confirm the strong damping (Figure 5).

Figure 5 Left: 12 K cooler cold head temperature spectrum, it is evident the main 1Hz frequency (from AD1). Right: the corresponding spectrum at the level of the Band 6 cartridge (from AD1).
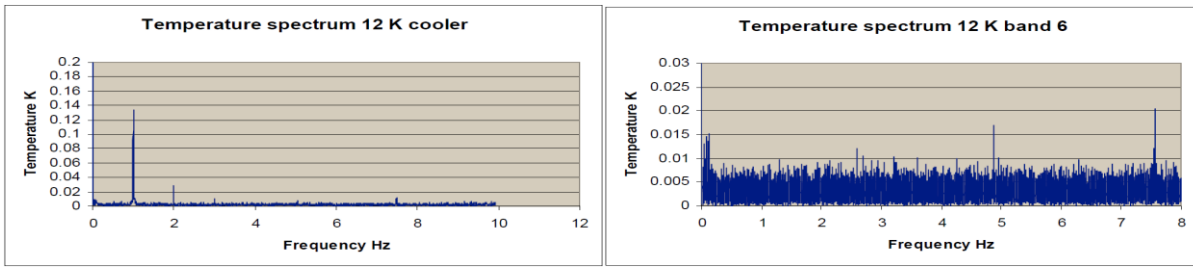
However, a simulation has been run to check the impact of 1 Hz fluctuation on the sensitive part of the cartdridge design under study. Starting from the original spectra of the cooler a temperature curve was built and associated to the 18 K flange of our cartridge. We studied how this fluctuation propagates to the central region of the front end module, where LNAs would be located.
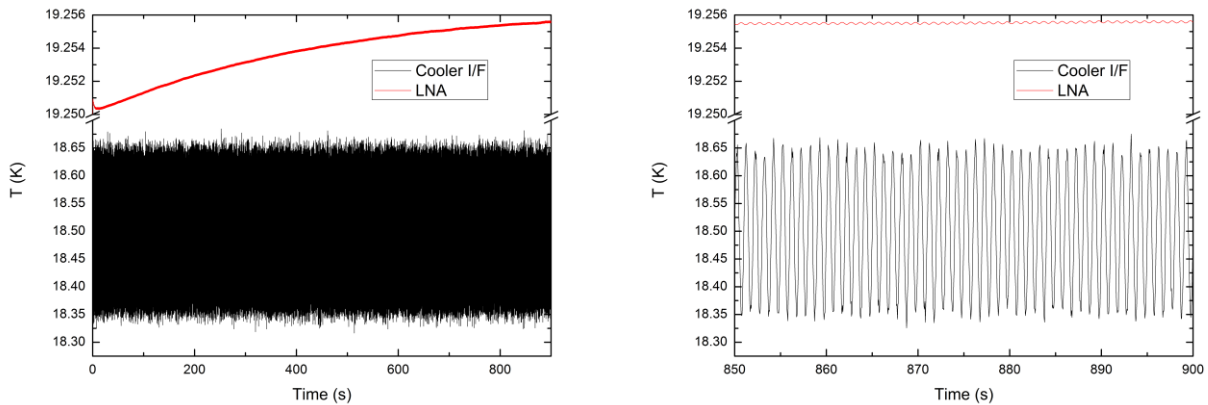

Figure 6 Left: overview of the results of a simulation where a 150 mK fluctuation at 1 Hz is entered at the level of the cartridge 18 K stage interface and the corresponding temperature curve in the receiver front end is observed. Right: a zoom on the final part of the curves.

As expected the instability is strongly reduced and it becomes up to 500 times smaller (Figure 6).

On larger time scales, slow drifts can be optimally treated by adding an active control stage.

Taking into account the current thermal conductance, 0.05 W/K between the device and the 18 K flange interface, it can be easily evaluated that the residual heat lift available of 26 mW can be used to compensate drifts of about 0.5 K on medium timescales. This would allow to keep the receiver as stable as desired keeping the temperature still under 20 K.

It is also important to notice that the cold optics connected to the feed horn mount would benefit of this stability, as well. An estimation of a few mK impact on the signal measured from a physical temperature fluctuation of 2 K in the optics, if located at room temperature, is discussed in the Optical System report and shortly described here in the Appendix 10.2. A stability at a level of three order of magnitude better would then mean that it is a completely negligible effect.

9 Summary and conclusions

The thermal setup of a Band 2+3 cartridge to be implemented in the ALMA cryostat has been studied.

The cartridge proposed is taking advantage of the two warmer stages of the cryostat cooler, in the 12 K stage the optical and sensitive parts of the instruments are located, while the intermediate 90 K stage

as a transition phase to the warm back end part, radiatively protecting the cold part and also creating a break in the conductive dissipation.

This study found no crytical issue in the cryogenic implementation of the proposed cartridge scheme in term of particular thermal control system solutions.

The use of standard materials and structures is considered feasible.

A close interaction with the detector and the optical team would of course be needed in the phase of finalization of the design, as the amplifier dissipation and the transmission of thermal control devices are the key interface thermal parameters.

10 Appendix

10.1 Thermal model nodes setup

In the table below the thermal model nodes are reported, together with the absolute temperature reached at the steady state and the heat balance obtained. In the case of boundary nodes, i.e. environment cryostat walls and cooler interfaces the heat balance corresponds to the total heat absorbed or released by the stage.

Node #	Label	T steady (K)	Heat Balance (W)
Node:20	Top_20K	18.85	2.01E-09
Node:50	Horn	19.26	2.84E-11
Node:55	Horn_Base	19.26	8.18E-13
Node:56	Horn_Base	19.26	7.47E-13
Node:80	Top_80K	105.20	1.42E-08
Node:100	HornFlange2	19.26	-1.07E-14
Node:101	HornFlange1	19.26	4.30E-12
Node:120	base_cyl	19.26	5.66E-13
Node:150	M1	19.26	7.71E-12
Node:250	M2	19.26	3.38E-11
Node:300	Flange_Cryo300	290.00	-4.276
Node:301	Flange_Cryo300	290.00	0.424
Node:302	Flange_Cryo300	290.00	-0.155
Node:303	Flange_Cryo300	290.00	-0.154
Node:390	Flange_Cryo300	290.00	0.006
Node:391	Flange_Cryo300	290.00	0.001
Node:392	Flange_Cryo300	290.00	-0.12
Node:393	Flange_Cryo300	290.00	-0.118
Node:394	Flange_Cryo300	290.00	0.001
Node:395	Flange_Cryo300	290.00	0.007
Node:397	Flange_Cryo300	290.00	0.07
Node:398	Flange_Cryo300	290.00	-0.006
Node:399	Flange_Cryo300	290.00	-0.051
Node:500	Cold_Support	34.65	2.62E-08
Node:501	Cold_Support	62.47	-4.74E-09
Node:502	Cold_Support	84.31	-4.73E-09
Node:505	Cold_Support	34.65	2.62E-08

Node:506	Cold_Support	62.47	-4.68E-09
Node:507	Cold_Support	84.31	-4.83E-09
Node:550	Warm_Support	171.50	7.46E-06
Node:551	Warm_Support	225.50	4.50E-06
Node:552	Warm_Support	256.80	5.54E-06
Node:555	Warm_Support	171.60	7.51E-06
Node:556	Warm_Support	225.50	4.48E-06
Node:557	Warm_Support	256.80	5.52E-06
Node:700	Shield_20K	18.80	2.07E-08
Node:701	Shield_20K	18.80	1.79E-08
Node:720	Lid_20K	18.84	1.08E-09
Node:721	Lid_20K	18.84	6.65E-09
Node:722	Lid_20K	18.84	9.83E-09
Node:723	Lid_20K	18.84	1.34E-08
Node:740	Base_20K	18.66	1.14E-09
Node:741	Base_20K	18.68	8.35E-09
Node:742	Base_20K	18.69	1.45E-08
Node:743	Base_20K	18.70	2.00E-08
Node:760	Flange_20K	18.50	0.164
Node:761	Flange_20K	18.50	0.001
Node:762	Flange_20K	18.50	0.816
Node:763	Flange_20K	18.50	0.04
Node:800	Shield_100K	102.10	8.37E-07
Node:801	Shield_100K	102.30	2.90E-07
Node:820	Top_100K	104.30	3.20E-09
Node:821	Top_100K	104.20	4.16E-08
Node:822	Top_100K	104.10	7.42E-08
Node:840	Base_100K	98.59	1.58E-07
Node:841	Base_100K	98.87	6.26E-07
Node:842	Base_100K	99.06	1.02E-06
Node:860	Flange_90K	95.00	-0.001
Node:861	Flange_90K	95.00	-0.001
Node:862	Flange_90K	95.00	8.832
Node:900	Cryostat	290.00	-0.489
Node:901	Cryostat	290.00	-0.45
Node:902	Cryostat	290.00	-0.399
Node:903	Cryostat	290.00	-0.32
Node:920	Cryo_Base	290.00	-0.009
Node:921	Cryo_Base	290.00	-0.148
Node:922	Cryo_Base	290.00	-0.242
Node:923	Cryo_Base	290.00	-0.343
Node:940	Cryo_Lid	290.00	-0.016
Node:941	Cryo_Lid	290.00	-0.077
Node:942	Cryo_Lid	290.00	-0.144
Node:943	Cryo_Lid	290.00	-0.204
Node:963	Flange_90K	95.00	-0.796

Node:2000	FEM	19.26	1.07E-11
Node:2001	FEM	19.25	2.04E-12
Node:2002	FEM	19.26	2.02E-12
Node:2003	FEM	19.26	2.25E-12
Node:2004	FEM	19.26	2.20E-12
Node:2005	FEM	19.26	2.08E-12
Node:2006	FEM	19.25	2.88E-12
Node:2007	FEM	19.26	2.65E-12
Node:2008	FEM	19.26	3.13E-12
Node:2009	FEM	19.26	3.31E-12
Node:2010	FEM	19.26	3.83E-12
Node:2011	FEM	19.25	1.84E-12
Node:2012	FEM	19.26	2.03E-12
Node:2013	FEM	19.26	1.97E-12
Node:2014	FEM	19.26	1.94E-12
Node:2015	FEM	19.26	1.89E-12
Node:2016	FEM	19.25	2.96E-12
Node:2017	FEM	19.26	2.89E-12
Node:2018	FEM	19.26	2.62E-12
Node:2019	FEM	19.26	2.79E-12
Node:2020	FEM	19.26	2.99E-12
Node:2021	FEM	19.25	1.30E-11
Node:3020	Filter_20K	19.07	9.17E-10
Node:3021	Filter_20K	18.85	2.54E-09
Node:3100	Filter_100K	131.90	8.59E-09
Node:3101	Filter_100K	105.70	2.76E-08
Node:3300	Win_Filter	290.00	-0.101
Node:3301	Win_Filter	290.00	-0.269
Node:3302	Win_Filter	290.00	-0.532
Node:9999	Environment	300.00	-0.255
Node:10000	Environment	300.00	-0.088
Node:10001	Environment	300.00	-0.091
Node:10002	Environment	300.00	-0.088
Node:10003	Environment	300.00	-0.087
Node:10004	Environment	300.00	-0.291
Node:99999	ENVIRONMENT	300.00	0

10.2 Impact of cold optics

An extimation of the benefits of keeping the optics in the cold stage inside the cryostat was performed. The additional noise temperature caused by the reflectors can be evaluated from:

$$\frac{\Delta T_N}{T_{sys}} = (L - 1)\left(\frac{T_{phys}}{T_{sys}} + 1\right)$$ where the loss is obtained as the product of the single contributions as we

assume, in our case, that the two reflectors have identical properties and temperature:

$$L = \left(\cfrac{1}{1 - 4\sqrt{\cfrac{\pi \varepsilon_0 \nu}{\sigma}}} \right)^2$$, and it is a function of the frequency ν and the electrical conductivity of the

material σ, which is also dependent on temperature. As evident from the equations the relative change of noise temperature is directly linked to the physical temperature of the reflectors, so that having them at room temperature or inside the cryostat create one order of magnitude difference. We report the values we estimated in the Table below. The last column reports the results of a further exercise we performed to evaluate the effect of the intrinsic instability of having the small mirrors outside the cryostat controlled environment: we evaluated the fluctuation in the antenna temperature measured from the instrument (assumed with a worst case of 50 K system temperature) caused by a variation of 2 K in the physical temperature of the mirrors.

Freq [GHz]	dT_N/T_{sys} (15K)	dT_N/T_{sys} (300K)	dT_{ant} (K)
67	0.001672	0.015534	4.44E-03
68	0.001684	0.015650	4.47E-03
69	0.001697	0.015765	4.50E-03
70	0.001709	0.015879	4.54E-03
71	0.001721	0.015992	4.57E-03
72	0.001733	0.016104	4.60E-03
73	0.001745	0.016216	4.63E-03
74	0.001757	0.016327	4.66E-03
75	0.001769	0.016437	4.70E-03
76	0.001781	0.016546	4.73E-03
77	0.001792	0.016655	4.76E-03
78	0.001804	0.016763	4.79E-03
79	0.001815	0.016870	4.82E-03
80	0.001827	0.016977	4.85E-03
81	0.001838	0.017083	4.88E-03
82	0.001850	0.017188	4.91E-03
83	0.001861	0.017293	4.94E-03
84	0.001872	0.017397	4.97E-03
85	0.001883	0.017501	5.00E-03
86	0.001894	0.017603	5.03E-03
87	0.001905	0.017706	5.06E-03
88	0.001916	0.017807	5.09E-03
89	0.001927	0.017908	5.12E-03
90	0.001938	0.018009	5.15E-03
91	0.001949	0.018109	5.17E-03
92	0.001959	0.018208	5.20E-03
93	0.001970	0.018307	5.23E-03
94	0.001981	0.018406	5.26E-03
95	0.001991	0.018503	5.29E-03
96	0.002001	0.018601	5.31E-03
97	0.002012	0.018698	5.34E-03

98	0.002022	0.018794	5.37E-03
99	0.002033	0.018890	5.40E-03
100	0.002043	0.018985	5.42E-03
101	0.002053	0.019080	5.45E-03
102	0.002063	0.019174	5.48E-03
103	0.002073	0.019268	5.51E-03
104	0.002083	0.019362	5.53E-03
105	0.002093	0.019455	5.56E-03
106	0.002103	0.019547	5.58E-03
107	0.002113	0.019640	5.61E-03
108	0.002123	0.019731	5.64E-03
109	0.002133	0.019823	5.66E-03
110	0.002143	0.019914	5.69E-03
111	0.002152	0.020004	5.72E-03
112	0.002162	0.020094	5.74E-03
113	0.002172	0.020184	5.77E-03
114	0.002181	0.020273	5.79E-03
115	0.002191	0.020362	5.82E-03
116	0.002200	0.020451	5.84E-03